JCTC Journal of Chemical Theory and Computation

A Barrier-Free Atomic Radical-Molecule Reaction: F + Propene

Ji-Lai Li, Cai-Yun Geng, Xu-Ri Huang,* and Chia-Chung Sun

State Key Laboratory of Theoretical and Computational Chemistry, Institute of Theoretical Chemistry, Jilin University, Changchun 130023, People's Republic of China

Received September 18, 2005

Abstract: The possible reaction mechanism of atomic radical F with propene is investigated theoretically by a detailed potential energy surface (PES) calculation at the UMP2/6-311++G-(d,p) and CCSD(T)/cc-pVTZ (single-point) levels using ab initio quantum chemistry methods and transition-state theory. Various possible reaction paths including addition−isomerization−elimination reactions and direct H-atom abstraction reactions are considered. Among them, the most feasible pathway should be the atomic radical **F** (^{2}F) attacking on the C═C double bond in propene ($CH_3CH{=}CH_2$) to form a weakly bound complex **I1** with no barrier, followed by atomic radical **F** addition to the C═C double bond to form the low-lying intermediate isomer 3 barrierlessly. Starting from intermediate isomer 3, the most competitive reaction pathway is the dissociation of the C2−C3 single bond via transition state **TS3**−**P5**, leading to the product **P5**, CH_3 + $CHF{=}CH_2$. However, in the direct H-atom abstraction reactions, the atomic radical **F** picking up the *b*-allylic hydrogen of propene barrierlessly is the most feasible pathway from thermodynamic consideration. The other reaction pathways on the doublet PES are less competitive because of thermodynamical or kinetic factors. No addition−elimination mechanism exists on the potential energy surface. Because the intermediates and transition states involved in the major pathways are all lower than the reactants in energy, the title reaction is expected to be rapid. Furthermore, on the basis of the analysis of the kinetics of all channels through which the addition and abstraction reactions proceed, we expect that the competitive power of reaction channels may vary with experimental conditions for the title reaction. The present study may be helpful for probing the mechanisms of the title reaction and understanding the halogen chemistry.

1. Introduction

The reactivity of the fluorine atom is an interesting research topic because of the complicated nature of the reaction mechanism involved in these reactions and its importance in many industrial applications. A variety of reaction mechanisms are involved in its reaction with different molecules. The reactions of fluorine atoms with unsaturated hydrocarbons have been studied, both theoretically and experimentally.[1−16] It was found that this class of reactions proceeds primarily by the addition of fluorine atoms to the double bond of the hydrocarbon molecules to form long-lived chemical-activated radical complexes, which further decompose unimolecularly to give predominantly hydrogen atoms or methyl radicals. In contrast, in the **F** atom reaction with methane,[17−20] the reaction mainly occurs through an abstraction mechanism to produce a HF molecule and a methyl radical (CH_3) in which the CH_3 part is largely a spectator during the reaction process. Recently, Lee and co-workers[5] carried out the crossed-beam study on the reaction dynamics of the F atom reaction with the propene molecule with both single and double bonds, in which reactions occur

* Corresponding author fax: (+86) 431-894-5942; e-mail: lijilai2008@yahoo.com.

10.1021/ct050233m CCC: $33.50
Published on Web 09/01/2006

through both direct abstraction and long-lived complex formation mechanisms. As shown in eqs 1−3, three different reaction channels of the $F + C_2H_3CH_3$ reaction have been identified: (1) the H atom formation channel takes place through some direct reaction mechanism and is likely to be a long-lived complex formation process; (2) the CH_3 formation process mainly proceeds through a long-lived complex formation mechanism, and (3) HF formation shows clearly that a direct pickup-type reaction mechanism is responsible for this channel. Experimental results show that the CH_3 formation is the most important reaction pathway for the title reaction, while both H and HF formation channels are also significant.

$$F + C_2H_3CH_3 \rightarrow C_3H_5F + H \quad (15\%) \qquad (1)$$

$$F + C_2H_3CH_3 \rightarrow C_2H_3F + CH_3 \quad (65\%) \qquad (2)$$

$$F + C_2H_3CH_3 \rightarrow C_3H_5 + HF \quad (19\%) \qquad (3)$$

However, Lee et al.[5] did not further provide unambiguous information on the site-specific effect in the H-atom elimination channels and the HF formation channels although there are three chemically different hydrogen sites in the propene molecule. This information may be important in the site specificity of the sequential chain processes. To the best of our knowledge, the nature of different reaction channels in the atomic radical **F** reactions with hydrocarbon molecules has not been investigated in detail in all previous experiments, and no report is found about the theoretical study on the title reaction. In addition, recently, Braña and Sordo have built up the potential energy surfaces (PESs) of the analogous **Cl + propene** reaction.[21] Now, the sequential question is whether the mechanism of the title reaction **F** + propene is similar to the **Cl + propene** reaction or not.

In view of their potential importance and the rather limited information on them, a detailedly theoretical study on the doublet potential energy surfaces (DPESs) of the title reactions is therefore very desirable. The objective of the present article is threefold: (1) provide the elaborated isomerization and dissociation channels on the C_3H_6F DPESs, (2) investigate the site-specific effect of the title reactions to assist further experiment identification, and (3) provide some useful insight into the mechanism of the **F** + hydrocarbons reaction. Some conclusions that are drawn in this article may be helpful to resolve the question mentioned above and for further experimental studies of this reaction.

2. Computational Method Details

All of the calculations reported in this work were carried out on SGI O3800 servers using the Gaussian 98 and 03 program packages.[22] Unless otherwise stated, all geometries of the reactants, complexes, intermediates, transition states (TSs), and products have been fully optimized with the unrestricted Møller−Plesset second-order perturbation UMP2-(FULL)[23] method using the 6-311++G(d,p) basis set. The presence of diffuse functions in the basis set allows for an appropriate representation of the dispersion forces that should play an important role in the stabilization of the weakly bound structures considered in this work.[24] Vibrational frequencies, also calculated at the same level of theory, have been used to characterize stationary points, zero-point energy (ZPE) corrections calculations. The number of imaginary frequencies for intermediates and transition states are 0 and 1, respectively. The ZPE and vibrational frequencies were scaled by a factor of 0.95 for anharmonicity correction.[25] To confirm that the transition states connect between designated intermediates, intrinsic reaction coordinate (IRC)[26] calculations were performed at the UMP2(FULL)/6-311++G-(d,p) level of theory.

For the purpose of obtaining more reliable energies of various structures, the coupled-cluster CCSD(T) method with single, double, and perturbative treatment of triple excitations[27] in conjunction with the correlation-consistent polarized valence triple-ζ basis sets cc-pVTZ[28] was used. The UMP2(FULL)/6-311++G(d,p) optimized geometries were used for the single-point coupled cluster calculations without reoptimization at the CCSD(T)/cc-pVTZ levels.

The major problem in the application of unrestricted single-determinant reference wave functions is that of contamination with higher spin states. The severe spin contamination could lead to a deteriorated estimation of the barrier height.[29,30] We have examined the spin contamination before and after annihilation for the radical species and transition states involved in the $F + C_2H_3CH_3$ reaction. For doublet systems, the expectation values of $\langle S^2 \rangle$ range from 0.98 to 0.75 before annihilation, and after annihilation, $\langle S^2 \rangle$ is 0.75∼0.76 (the exact value for a pure doublet is 0.75). This suggests that the wave function is not severely contaminated by states of higher multiplicity.[31, 32]

Recent studies on systems similar to the ones considered in this article concluded that the use of spin annihilation techniques to generate spin-projected energies is mandatory for calculations of both reaction energies and barrier heights.[33] All of the UMP2 energy values reported in this work correspond to spin-projected calculations (PMP2) to correct for spin contamination using Schlegel's algorithm.[34] On the other hand, Stanton has shown that all spin contamination is essentially removed from a coupled cluster wave function.[35] Considering that, even with modest spin contamination, the position and height of the barriers may be affected,[36] several points along the reaction path (IRC) were optimized at the UMP2 level, followed by single-point calculations at the CCSD(T) level to verify the negative barriers at the reactant entrance, because the reaction path should be less sensitive to spin contamination.[37] Therefore, we expect that the CCSD(T) calculations reported in this work are, in this regard, reliable.

The thermodynamic functions (ΔH, ΔS, and ΔG) were estimated within the ideal gas, rigid-rotor, and harmonic oscillator approximations. A temperature of 298.15 K and a pressure of 1 atm were assumed.

3. Results and Discussion

For the present C_3H_6F system, there are enantiomorphs. For convenient and clear discussion, we only present moieties of reaction channels that have enantiomorphic varieties and

some important enantiomorphous structures. Six intermediate complexes (loose structure), six intermediate isomers, 11 products, and 21 transition states are obtained at the UMP2-(FULL)/6-311++G(d,p) or UMP2(FULL)/6-311G level of theory. The structures of the reactants, intermediate complexes and isomers, transition states, and products are depicted in Figure 1. The symbol **TS*x*-*y*** is used to denote a transition state, where ***x*** and ***y*** are the corresponding isomers or products. By means of the interrelation among the reactants, complexes, isomers, transition states, and products as well as the corresponding relative energies, the schematic profiles of the potential energy surface are depicted as shown in Figure 2. The schematic map of reaction mechanisms and activation energies of the title reaction is shown in Scheme 1. The direct H-abstraction manners are shown in Scheme 2. The calculated energetic data (ΔE, ΔH, ΔS, and ΔG) of various products, complexes, isomers, and transition states and values obtained experimentally are listed in Table S1 as Supporting Information. It should be noted that the energy of **F + propene** is set at zero as a reference for other species for convenient discussion. As shown in Table S1, it is clear that the results calculated at the CCSD(T)/cc-pVTZ//UMP2-(FULL)/6-311++G(d,p) level of theory are in good agreement with the experimental values. Some apparent inconsistencies appearing in Figure 2 and in Table S1 in this work arise from the use of single-point spin-projected energies[34] (see, e.g., in Figure 2a, where **TS1−3** lies 2.27 kcal/mol below **I1**, etc.). We checked that all of the unprojected energy profiles are topologically consistent. In addition, the harmonic vibrational frequencies of some important species are given in Table S2 as Supporting Information. A comparison between the theoretical results and available experimental data for the reactant propene, product HF, C_2H_3F, and C_2H_4 is also presented in Table S2 (Supporting Information).

3.1. Analysis of Reaction Mechanism of Atomic Radical F with Propene. As the atomic radical **F•** ("•" denotes the unpaired single electron) can have either a direct abstraction or an addition mechanism, two distinguishable types of initial attacks have been revealed for the radical-molecule reaction **F + propene**, namely, the picking-up on hydrogen (direct hydrogen abstraction) and the attack on the C=C double bond (addition−isomerization−elimination). A detailed discussion on the title reaction mechanisms as shown in Figure 2 is given as follows.

3.1.A. Addition−Isomerization−Elimination Reaction Mechanism. First, the atomic radical **F** (^{2}F) and propene (CH_3-CH=CH_2) approach each other forming a weakly bound complex **1** (**I1**). Complex **1** contains two C···F bonds (see Figure 1), which stabilize the complex by 9.30 kcal/mol relative to the reactant **R**, F + CH_3CH=CH_2 (0.0 kcal/mol). It is obvious that this addition process is a barrier-free association.[15,21] Then, complex **1** can undergo two concerted three-center F shifts; one of the F shifts is the C1···F bond being shortened and the C2···F bond being elongated (**TS1−2**) to produce the low-lying intermediate isomer **2**, CH_3-$CHCHF$ (**I2**, −42.65), with large exothermicity, while the other is the C1···F bond being elongated and the C2···F bond being shortened, leading to another low-lying intermediate isomer **3**, CH_3CFCH_2 (**I3**, −43.96), with larger exothermicity. The **I1** → **I2** and **I1** → **I3** energy barriers are negative, −2.11 and −2.27 kcal/mol, respectively, at the CCSD(T)/cc-pVTZ//UMP2/6-311++G(d,p) level of theory. IRCMax-(CCSD(T)//UMP2)[37] calculations confirmed these connections, in which **TS1−3** and **TS1−2** lie −1.13 and −1.28 kcal/mol lower in energy than I1, respectively. As was indicated earlier, most radical additions to the unsaturated carbon−carbon double bond have negative activation barriers.[15,21] Thus, the presence of **I1** on the PES is mandatory, for the topological consistency of the PES of the title reaction. To our knowledge, it is the first time that the existence of a prereactive complex in the title reactions has been reported.

The overall processes **R** → **I1** → **I2** and **R** → **I1** → **I3** are both associated with the addition of the atomic radical **F** to the C=C double bond of CH_3CH=CH_2. They are typical **F**-addition mechanisms due to the electron-rich double bond in propene and the strong electronegativity of the F atom. As shown in Figure 1, the structural features of the addition transition states **TS1−2** and **TS1−3** are more similar to those of complex **1** than those of isomers **2** and **3**, respectively. It is consistent with the Hammond postulate, which states that a transition state will be structurally and energetically similar to the species (reactant, intermediate, or product) nearest to it on the reaction path. This is also in good agreement with the conclusion obtained by Yang and Zhang,[15] who have employed the molecular intrinsic characteristic contour and the electron density map methods.

With a large amount of heat released from the addition processes, isomers **2** and **3** can easily undergo 10 isomerization and dissociation pathways that can be expressed as follows:

Path1 RP5: **R** ^{2}F + CH_3CH=CH_2 → **I1** CH_3H $(C\cdots F\cdots C)_{ring}H_2$ → **I3** CH_3CHFCH_2 → **P5** CH_3 + CHF=CH_2

Path2 RP5: **R** → **I1** → **I2** CH_3CHCH_2F → **I6** *cis*-CH_3CH_2CHF → **P5**

Path3 RP5: **R** → **I1** → **I2** → **I5** *trans*-CH_3CH_2CHF → **P5**

Path4 RP7: **R** → **I1** → **I3** → **P7** H + CH_3CF=CH_2

Path5 RP7: **R** → **I1** → **I3** → **I7** CH_3CFCH_3 → **P7**

Path6 RP8: **R** → **I1** → **I2** → **P8** H + *cis*-CH_3CH=CHF

Path7 RP9: **R** → **I1** → **I2** → **P9** H + *trans*-CH_3CH=CHF

Path8 RP10: **R** → **I1** → **I2** → **P10** H + *cis*-CH_2=$CHCH_2F$

Path9 RP11: **R** → **I1** → **I2** → **P11** H + *trans*-CH_2=$CHCH_2F$

Path10 RP6: **R** → **I1** → **I2** → **I4** → **P6** CH_2F + CH_2=CH_2

In terms of small species in products, the title reaction has three different channels in the addition−isomerization−elimination reaction mechanism, that is, (I) the CH_3 radical formation channels, paths 1−3; (II) the H-atom formation channels, paths 4−9; and (III) the CH_2F radical formation channels, that is, path 10.

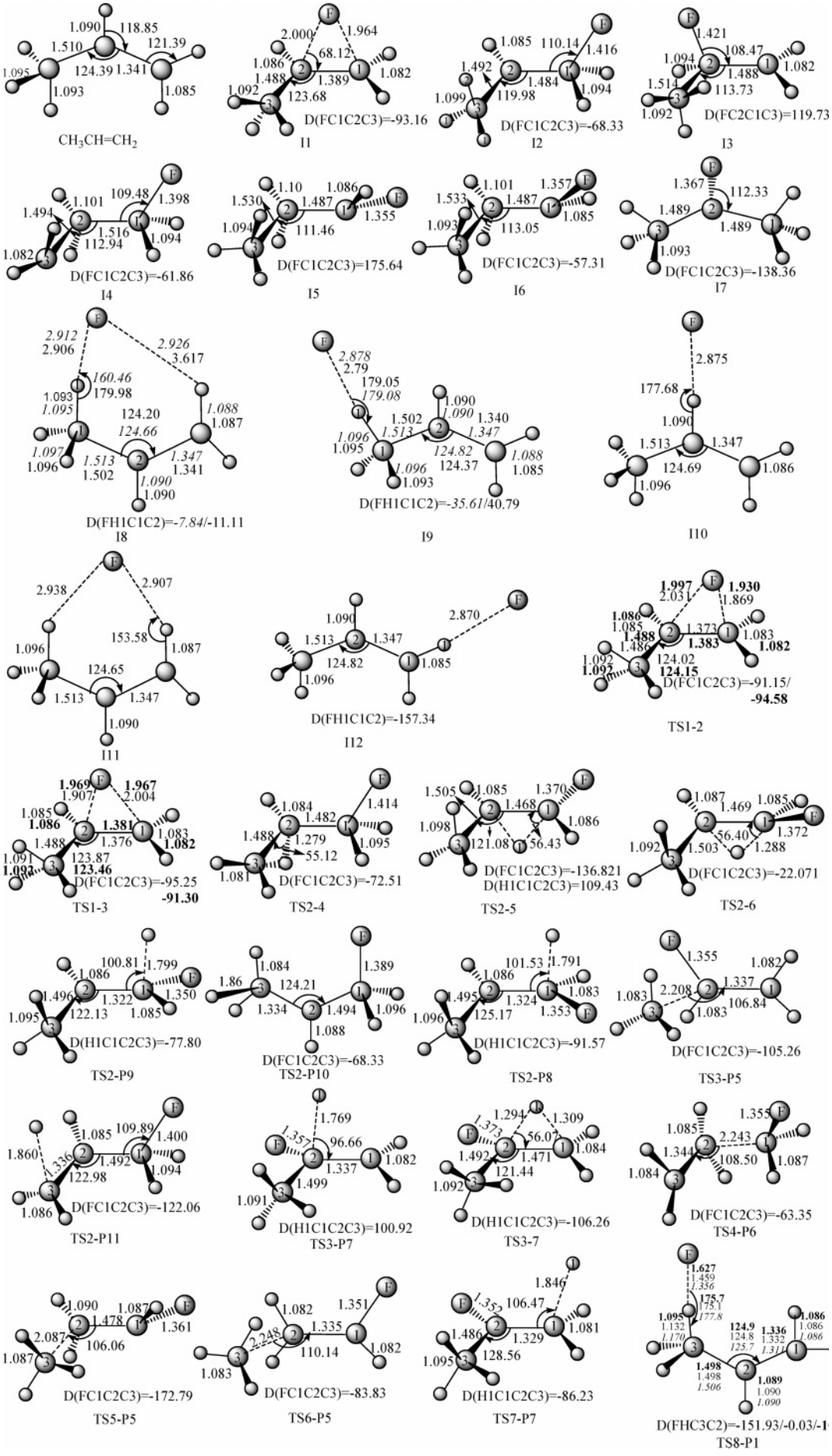
CH3CH=CH2
D(FC1C2C3)=-93.16
I1
D(FC1C2C3)=-68.33
I2
D(FC2C1C3)=119.73
I3
D(FC1C2C3)=-61.86
I4
D(FC1C2C3)=175.64
I5
D(FC1C2C3)=-57.31
I6
D(FC1C2C3)=-138.36
I7
D(FH1C1C2)=-7.84/-11.11
I8
D(FH1C1C2)=-35.61/40.79
I9
I10
D(FH1C1C2)=-157.34
I12
D(FC1C2C3)=-91.15/
-94.58
TS1-2
D(FC1C2C3)=-95.25
-91.30
TS1-3
D(FC1C2C3)=-72.51
TS2-4
D(FC1C2C3)=-136.821
D(H1C1C2C3)=109.43
TS2-5
D(FC1C2C3)=-22.071
TS2-6
D(H1C1C2C3)=-77.80
TS2-P9
D(FC1C2C3)=-68.33
TS2-P10
D(H1C1C2C3)=-91.57
TS2-P8
D(FC1C2C3)=-105.26
TS3-P5
D(FC1C2C3)=-122.06
TS2-P11
D(H1C1C2C3)=100.92
TS3-P7
D(H1C1C2C3)=-106.26
TS3-7
D(FC1C2C3)=-63.35
TS4-P6
D(FC1C2C3)=-172.79
TS5-P5
D(FC1C2C3)=-83.83
TS6-P5
D(H1C1C2C3)=-86.23
TS7-P7
D(FHC3C2)=-151.93/-0.03/-1
TS8-P1

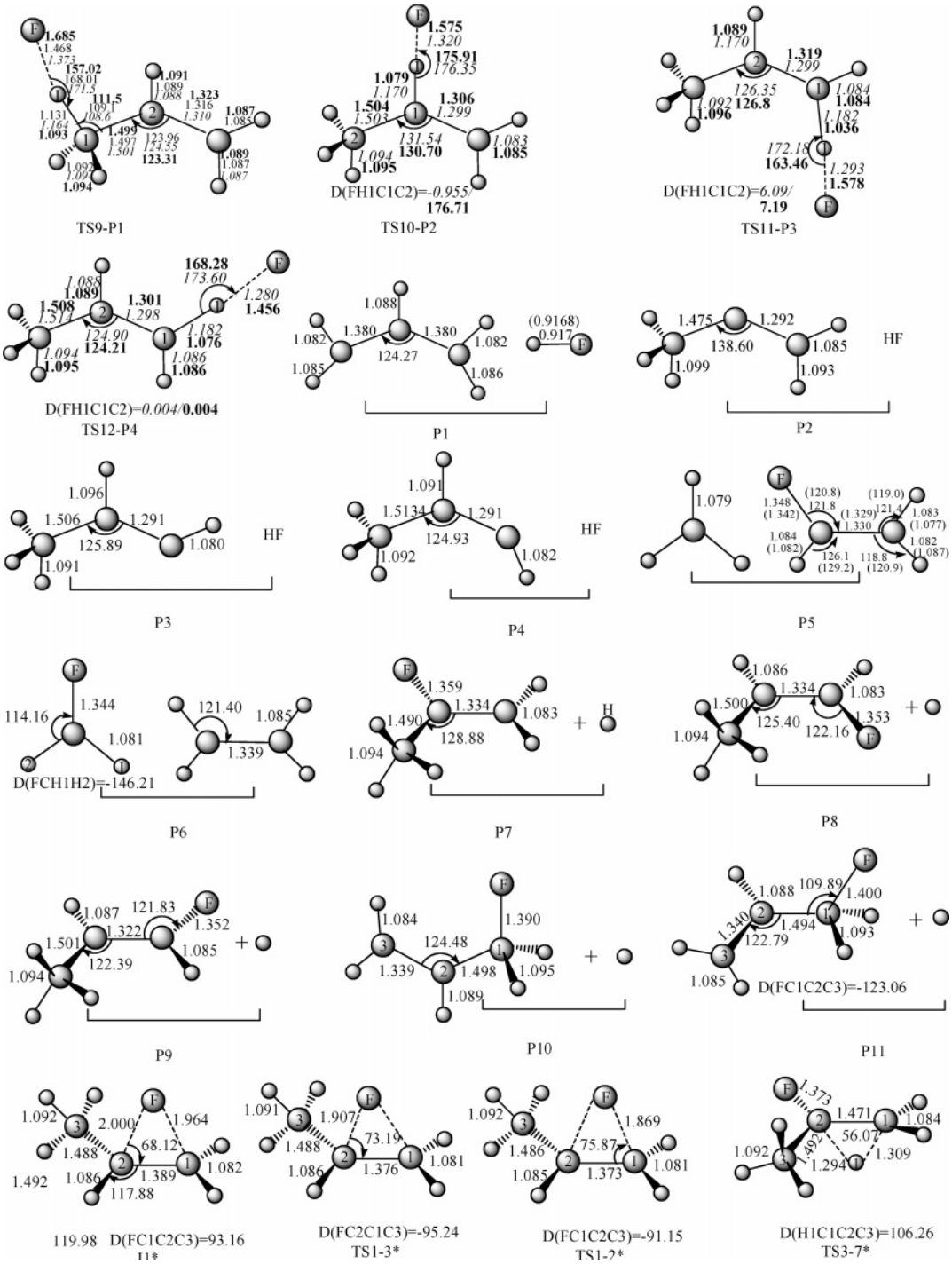

Figure 1. Optimized geometries of the reactants, the complexes, the doublet intermediate isomers, the products, and the transition states for the F + propene reaction. Bond distances are in angstroms, and angles are in degrees. Numbers in roman type show the structures at the UMP2/6-311++G(d,p) level of theory. Numbers in italics show the structures at the UMP2/6-311G level of theory. Numbers in bold show the structures at the Max{CCSD(T)}//IRC{UMP2} + ZPE level of theory. Numbers in parentheses are the experimental values (ref 38 for HF, ref 39 for CH_2═CHF). Symbols with asterisks indicate enantiomorphic varieties corresponding to the same symbols.

3.1.A.I. The CH_3 Radical Formation Channel. Clearly, from complex **1**, $CH_3H(C\cdots F\cdots C)_{ring}H_2$ (−9.30), the pathway Path1 RP5 can reach the products **P5**, CH_3 + CHF═CH_2, easily by going through transition state **TS1**−**3** (−10.58), intermediate isomer **I3**, CH_3CHFCH_2 (−43.96), and **TS3**−**P5** (−10.45). As shown in Figure 1, the geometry of transition state **TS3**−**P5** calculated at the UMP2/6-311++G(d,p) level is found to have an elongated C2···C3 bond length (r_{C2-C3} = 2.208 Å). Most importantly, this geometry is indicative of a "late" transition state, corresponding to a C−C distance significantly longer than the equilibrium bond length (1.510 Å in propene). Because all of the energies of the transition states and isomers in pathway Path1 RP5 are lower than that of the reactants, the rate of this pathway should be very fast. Furthermore, because the pathway Path1 RP5 has no transition state in the first reaction step and tight structure

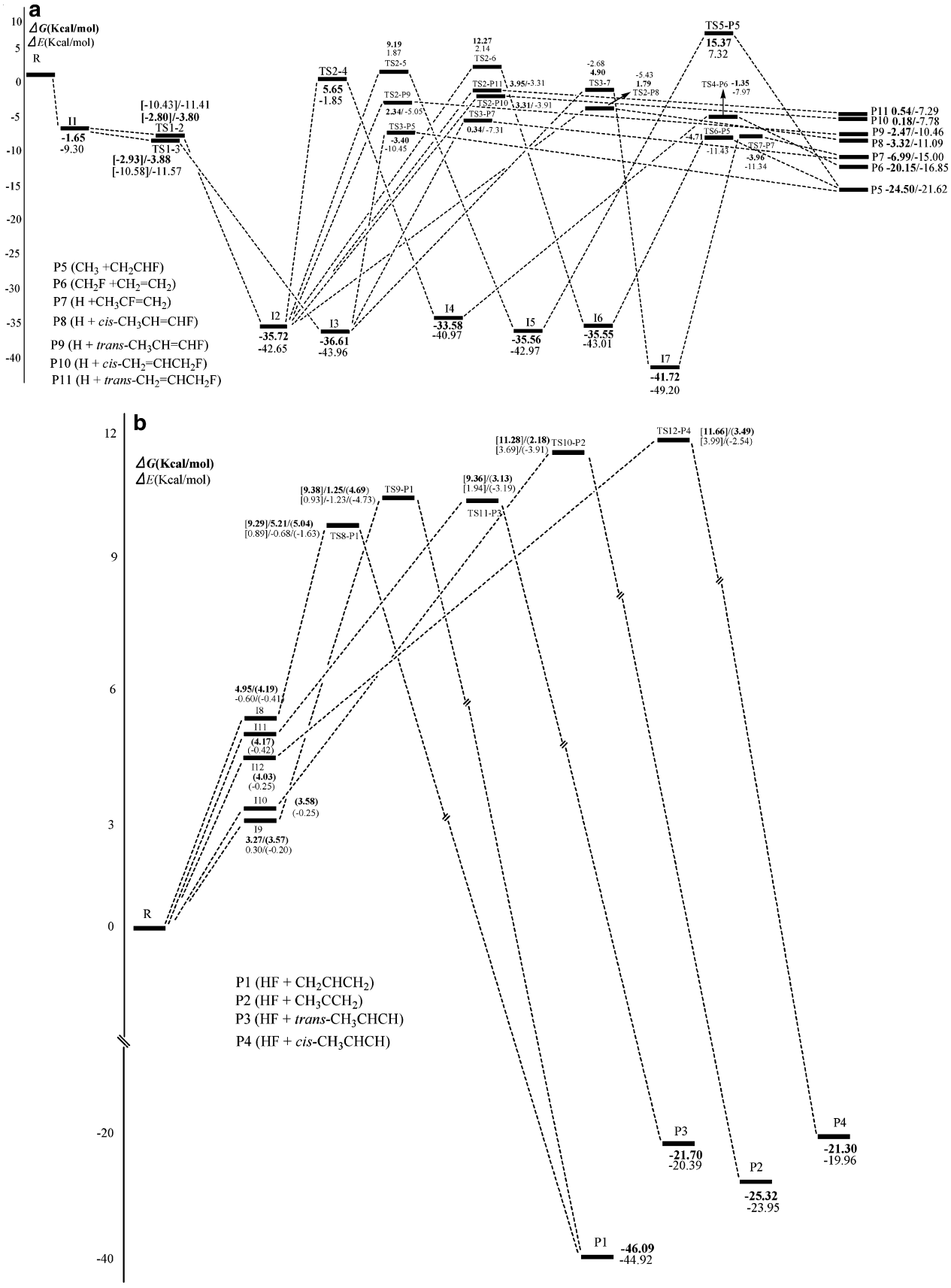

Figure 2. (a) Schematic potential energy surfaces of the addition−isomerization−elimination channels in the F + propene reaction. (b) Schematic potential energy surfaces of the hydrogen abstraction channels in the F + propene reaction. Numbers in roman type are relative energies at the CCSD(T)/cc-pVTZ//UMP2/6-311++G(d,p) + ZPE level of theory. Numbers in bold are relative Gibbs energies at the CCSD(T)/cc-pVTZ//UMP2/6-311++G(d,p) + ZPE level of theory. Numbers in parentheses are values at the CCSD(T)/cc-pVTZ//UMP2/6-311G + ZPE level of theory. Numbers in square brackets are values at the Max-{CCSD(T)}//IRC{UMP2} + ZPE level of theory.

Scheme 1. Reaction Mechanism and Activation Energies (kcal/mol) of the Reaction of F with Propene[a]

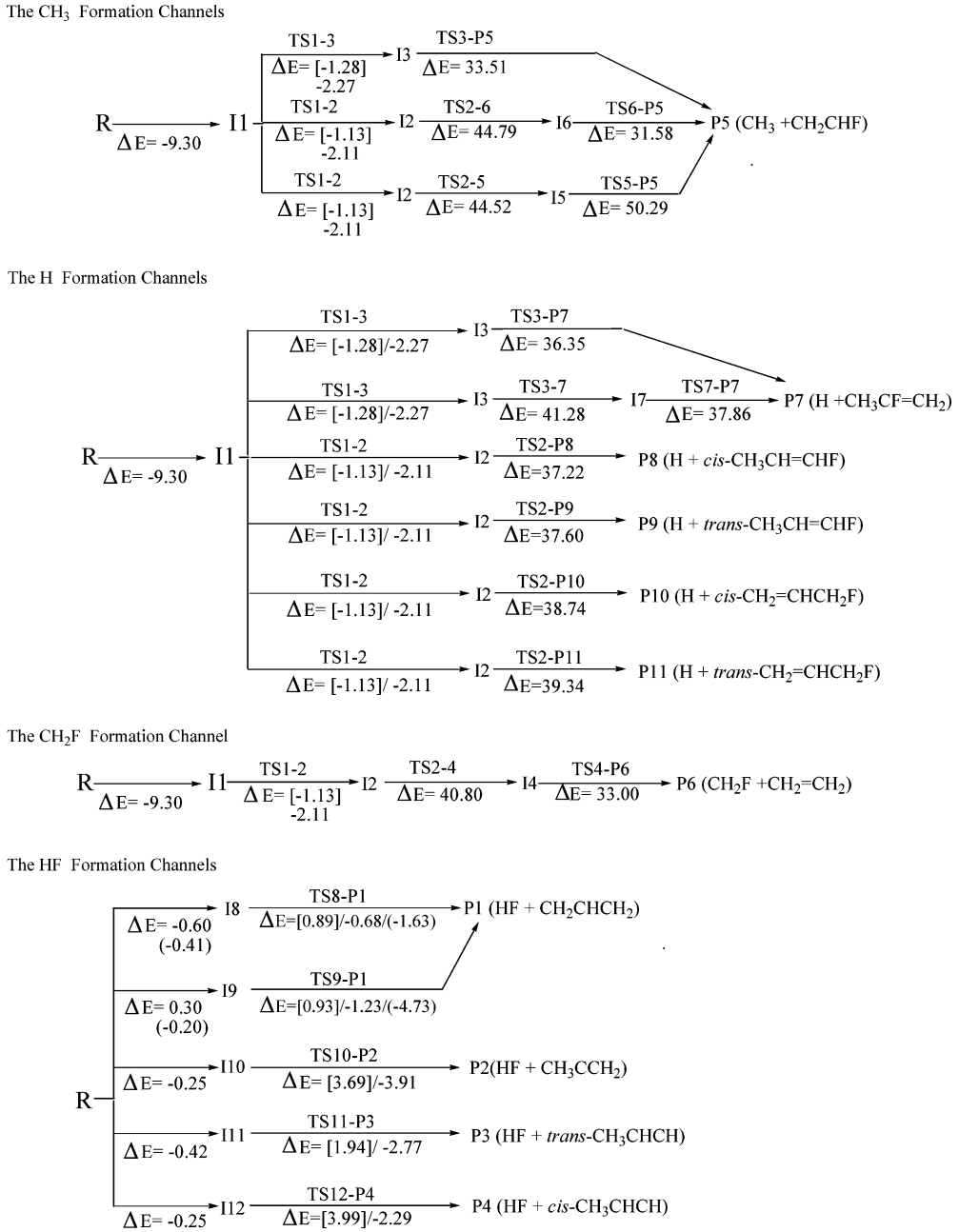

[a] Activation energies are calculated at the CCSD(T)/cc-pVTZ//UMP2/6-311++G(d,p) + ZPE (numbers in roman type), CCSD(T)/cc-pVTZ//UMP2/6-311G + ZPE (numbers in parentheses), and Max{CCSD(T)}//IRC{UMP2} + ZPE (numbers in square brackets) levels of theory.

isomers and transition states to the products, this pathway should possess the character of negative temperature dependence.

In pathway Path2 RP5, a successive 1,2-H-shift and dissociation steps **I2** → **I6** → **P5** can lead to product **P5**. It is an H-shift−methyl-elimination mechanism. Because the rate-determining energy barrier (44.79) of Path2 RP5 is higher than the ones of Path1 RP5 (33.51), pathway Path2 RP5 should be less competitive than pathway Path1 RP5. For Path3 RP5, similar successive 1,2-H-shifts and dissociation steps **I2** → **I5** → **P5** can also lead to product **P5**. As shown in Figure 1, the geometries of transition states **TS2**−**6** (2.14) and **TS2**−**5** (1.87) belong to a cis−trans configuration relationship and are energetically close and high-lying. Yet, the rather high energy barrier (50.29) of **TS5**−**P5** (7.32) makes the pathway Path3 RP5 process thermodynamically prohibited and far from competitive with pathways Path1 RP5 and Path2 RP5 under normal conditions.

3.1.A.II. The H-Atom Formation Channel. There are two pathways (Path4 and Path5) through which complex **1** can transform to the product **P7**. As shown in Figure 1, the transition structure **TS3**−**7** in Path5 RP7 is a hydrogen migration transition state. The relative energy of **TS3**−**7** is 4.63 kcal/mol higher than that of **TS3**−**P7**. Both the relative energies of rate-determining transition states and the simplicity considerations support the viability of pathway Path4 RP7. On the other hand, it is obvious that pathway Path4 RP7 is similar to pathway Path1 RP5 because pathway Path4 RP7 has the same steps of **R** → **I1** → **I3** as pathway Path1 RP5. The difference of the two pathways is how intermediate

Scheme 2. The Five Different Chemical H Atoms in Propene and the Five Possible Direct Abstraction Manners in the HF Formation Channel

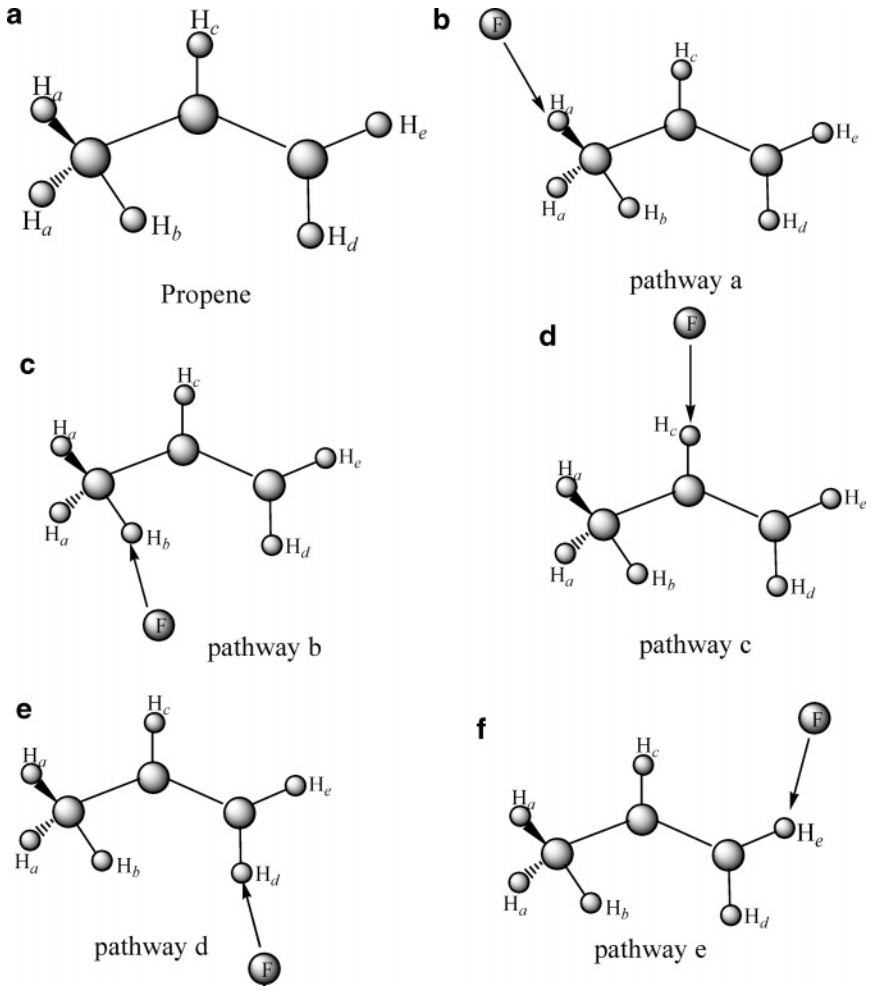

isomer **3** dissociates to relevant educts. In pathway Path1 RP5, **I3** can reach the product **P5** via surmounting the transition state **TS3**−**P5** (−10.45), a 33.51 kcal/mol energy barrier, while in pathway Path4 RP7, **I3** dissociates via overcoming the transition state **TS3**−**P7** (−7.31), a 36.35 kcal/mol energy barrier, leading to the product **P7**. The difference of the two pathways may lead us to the fact that pathway Path4 RP7 is less competitive than pathway Path1 RP5.

For the other four pathways, Path6 through Path9, which have the same steps of **R** → **I1** → **I2**, complex **1** (−9.30) transforms to intermediate isomer **2** (−42.65) via transition state **TS1**−**2** (−10.43) jointly, and subsequently, isomer **2** transforms to four different couples of educts **P8**, H + *cis*-$CH_3CH{=}CHF$ (−11.09); **P9**, H + *trans*-$CH_3CH{=}CHF$; **P10**, H + *cis*-$CH_2{=}CHCH_2F$; and **P11** H + *trans*-$CH_2{=}CHCH_2F$ via **TS2**−**P8** (−5.43), **TS2**−**P9** (−5.05), **TS2**−**P10** (−3.91), and **TS2**−**P11** (−3.31) via surmounting 37.22, 37.60, 38.74, and 39.34 kcal/mol energy barriers, respectively. As shown in Figure 1, their difference is how intermediate isomer **2** transforms to four different couples of educts, that is, the H elimination of the four different chemical sites of the H atom from intermediate isomer **2** (site specificity). From the thermodynamic stability of products and the rate-determining reaction steps, we can safely draw the conclusion that, for the six pathways in the H-atom formation channel mentioned above, the order of reaction competition abilities is Path4 RP7 > Path6 RP8 > Path7 RP9 > Path8 RP10 > Path9 RP11 > Path5 RP7.

According to our calculations, an unambiguous conclusion can be drawn to give a rational interpretation of the site-specific effect in the H-atom formation channel. As shown in Figure 1, **TS3**−**P7**, **TS2**−**P8**, **TS2**−**P9**, **TS2**−**P10**, and **TS2**−**P11** are the C2−H elimination of **I3**, $CH_3CHF{=}CH_2$; the C1−H_t elimination of **I2**, $CH_3CH{=}CH_2F$; the C1−H_c elimination of **I2**; the C3−H1 elimination of **I2**; and the C3−H2 elimination of **I2**, respectively, where the subscripts "t" and "c" denote the trans and cis H atoms of C1−H of I2, respectively. Because the pathway Path4 RP7 is the most feasible pathway in the H-atom formation channel, $CH_3CF{=}CH_2$ may be the main contribution in the C_3H_5F product. The contributions of *cis*-$CH_3CH{=}CHF$, *trans*-$CH_3CH{=}CHF$, *cis*-$CH_2{=}CHCH_2F$, and *trans*-$CH_2{=}CHCH_2F$ decrease orderly in terms of the competition abilities of their pathways.

3.1.A.III. The CH_2F Radical Formation Channel. As shown in Figure 2a, the pathway Path10 RP6 is the only pathway leading to product **P6**, $CH_2F + CH_2{=}CH_2$, in the CH_2F radical formation channel. In pathway Path10 RP6, the characteristic steps are **I2** → **I6** → **P6**, $CH_2F + CH_2{=}CH_2$; a three-center H migration; and a C−C bond rupture process. We should mention that the C−C rupture process in the CH_2F radical formation channel is obviously different from

the C−C rupture processes in the CH_3 radical formation channel. The former process occurs between C2 and C1, while all of the latter processes occur between C2 and C3 in the C_3H_6F system as shown in Figure 1. In terms of the formation heat of the CH_2F radical formation channel being a few kilocalories per mole more than that of the H-atom formation channel and the relative energy of rate-determining transition state **TS2−4** (−1.85) lying above those of **TS3−P7** (−7.31), **TS2−P8** (−5.43), **TS2−P9** (−5.05), **TS2−P10** (−3.91), **TS2−P11** (−3.31), and **TS4−P6** (−7.97), we conjecture that the CH_2F radical formation channel is less favorable than the H-atom formation channel in low-temperature ranges, while the latter should be competitive with the former under high-temperature conditions. Thus, the actual feasibilities of these two channels may depend on the reaction conditions in the experiments.

To briefly summarize, the CH_3 radical formation channel is the most competitive reaction channel, while the CH_2F radical formation channel may be prohibited in low-temperature ranges among the three channels. The pathway Path1 RP5 is the most competitive pathway among all 10 of the pathways. The CH_2F radical formation pathway Path10 RP6 may be more favorable than the H-atom formation pathway Path6 RP8 and Path7 RP9 in high-temperature ranges on the doublet PESs.

Now, it is requisite to compare the addition−isomerization−elimination PES feature of the title reaction with that of the analogous reaction F + ethylene, a detailed theoretical investigation on the formation of the intermediate complex, and a subsequent unimolecular decomposition.[15] Theoretical calculations show that there exist both similarity and discrepancy. In general, the addition−isomerization−elimination PES features of the two analogous reactions are very similar. First, both reactions involve the same initial association pathway; that is, the fluorine atom approaches ethylene/propene, perpendicular to the C═C double bond, forming the prereactive complex directly at the reaction entrance. The prereactive complex transforms to the fluoroethyl/fluoropropyl radicals via the addition transition structures with no barrier. Second, both radicals, fluoroethyl and fluoropropyl, can eliminate the H atom directly via surmounting 37∼39 kcal/mol barriers or indirectly by intramolecular H shifts with 41∼45 kcal/mol barriers. Furthermore, by comparison of the minima and transition structures in F + propene with the counterpoints in F + ethylene, we can find that their relative energies as well as the barrier heights vary little. For instance, according to Zhang and Yang's calculations,[15] the relative energies of the prereaction complex (I_{add}), the addition transition state (TS_{add}), and the fluoroethyl radical (CH_2FCH_2) in F + ethylene reaction are −9.30, −11.68, and −41.49 kcal/mol at the CCSD(T)/aug-cc-pVDZ//CCSD/6-31G(d,p) + ZPE level, which are in good agreement with that of **I1** (−9.30), **TS1-3** (−11.57), **TS1-2** (−11.41), **I3** (−43.96), and **I2** (−42.65) in the C_3H_6 + F reaction at the CCSD(T)/cc-pVTZ//UMP2/6-311++G(d,p) + ZPE level. On the other hand, the main discrepancies lie in the two folds: (a) an F-shift transition structure exists on the PES of F + ethylene, while it cannot be located on that of F + propene, and (b) the reaction pathways and possible products of F + propene are more than that of F + ethylene. It is obvious that the reaction of F + propene involves all of the main features of the F + ethylene reaction. However, from the discussion above, one can find that the addition−isomerization−elimination PES of F + propene is more complicated than that of F + ethylene because a hydrogen atom of ethylene is substituted by methyl in propene.

3.1.B. Direct Hydrogen Abstraction Reaction Mechanism. Scheme 2 shows the five possible pathways through which the abstraction reaction proceeds. For $CH_3CH{=}CH_2$, there are five different chemical environments of the H atom, namely, allylic hydrogen (H_a and H_b), vinyl inner hydrogen (H_c), and vinyl terminal hydrogen (H_d and H_e) as shown in Scheme 2. Pathways a and b correspond to the abstraction of the two nonequivalent allylic hydrogens. In pathway c, the vinyl inner hydrogen is the one involved in the abstraction reaction, whereas pathways d and e represent the abstraction of the vinyl terminal hydrogen. For convenient discussion, we list them as follows:

Path11 RP1: **R** → **I8** → **P1** HF + CH_2CHCH_2

Path12 RP1: **R** → **I9** → **P1**

Path13 RP2: **R** → **I10** → **P2** HF + CH_3CCH_2

Path14 RP3: **R** → **I11** → **P3** HF + *trans*-CH_3CHCH

Path15 RP4: **R** → **I12** → **P4** HF + *cis*-CH_3CHCH

As shown in Figure 1, five loosely bonded intermediate complexes (**I8−I12**) prior to the formation of the transition states along the reaction coordinate are located in the first step of this mechanism involved in the atomic radical **F** attacking the H atom of propene. However, as shown in Figure 2b, all of the complex formation processes are endothermic at the CCSD(T)//MP2 level of theory. This implies that such complexes might be short-lived and not important on the PES[41] and can be safely ruled out. On the other hand, one can find that all five of the abstraction hydrogen processes involve negative barriers at CCSD(T)//MP2 levels. In contrast, the IRCMax method consistently gives positive barriers that differ from the CCSD(T)//MP2 levels by 3∼8 kcal/mol with sizable displacements along the reaction path ($0.6 < S < 1.2$, see Table S3, Supporting Information). We expect that large errors are due to poor transition state geometries and positions along the IRCs at a low level of theory and thus have considerable effects on the calculated energy barriers. Furthermore, the barriers involved are moderate ($\Delta E < 4$ kcal/mol; $\Delta G < 12$ kcal/mol), and the formations of the final products are exergonic ($\Delta G > -21$ kcal/mol). Therefore, both kinetic and thermodynamic considerations support the viability of such channels.

Let us now analyze the low-temperature limiting behavior. Figure 2b shows that the rate-determining barriers of the five hydrogen abstraction channels are less than 4 kcal/mol at 0 K, especially for allylic hydrogen abstraction (**TS8-P1** and **TS9-P1**, $\Delta E < 1$ kcal/mol). Therefore, such processes may proceed in low-temperature ranges (the existence of a small barrier cannot be discarded as the errors in the calculation

ZPE because, for complexes with very small barriers, ZPE corrections are problematic, where the harmonic approximation does not work properly).

In pathway Path11 RP1, corresponding to the direct abstraction from the *b*-allylic hydrogen of $CH_3CH{=}CH_2$ as shown in Figure 1 and Scheme 2, the geometry of transition state **TS8-P1** calculated at the UMP2/6-311++G(d,p) level of theory is found to have a bent structure ($\angle_{F-H-C} = 175.1°$) and an elongated H−F bond length ($r_{F-H} = 1.459$ Å; $r_{C-H} = 1.132$ Å). Most importantly, this geometry is indicative of an "early" transition state, corresponding to a H−F distance significantly longer than the equilibrium bond length (0.917 Å), specifically falling between the HF classical outer turning points of $v = 4$(1.318 Å) and $v = 5$(1.381 Å).[42] The calculated heat of formation at 0 K (−44.92 kcal/mol) is in good agreement with the experimental value (−48.4 kcal/mol).[5] As shown in Figure 2b, this hydrogen abstraction channel is an exergonic process globally ($\Delta E = -44.92$ kcal/mol), involving a small barrier ($\Delta E = 0.89$ kcal/mol) at the Max{CCSD(T)/cc-pVTZ}//IRC{UMP2/6-311++G(d,p)} + ZPE level of theory. Therefore, both kinetic and thermodynamic considerations support the viability of this channel.

The *a*-allylic hydrogen abstraction pathway Path12 RP1 is totally similar to that described above for *b*-allylic hydrogen abstraction. And the relative energy of **TS9-P1** (0.93) is only 0.04 kcal/mol higher than that of **TS8-P1** (0.89) at the Max{CCSD(T)//IRC{UMP2} level of theory. The hairlike difference of the two pathways may lead us to the fact that pathway Path12 RP1 is less favorable than pathway Path11 RP1 appreciably.

Pathways Path13 through Path15 (see Figure 1 and Scheme 2) correspond to the possible abstraction of the vinyl hydrogens of propene. We should mention that the three transition states **TS10-P2**, **TS11-P3**, and **TS12-P4** are located at the UMP2/6-311G level of theory. Despite numerous attempts, we cannot locate these transition states at the higher levels of theory UMP2/6-311G(d,p) and UMP2/6-311++G(d,p). As shown in Table S1 (Supporting Information), the energy barriers and products in pathways Path13 through Path15 are higher than those in pathways Path11 through Path12 RP1. Therefore, both kinetic and thermodynamic considerations may rule out the significance of pathways Path13 through Path15.

We should mention that we also reoptimized **TS8-P1** and **TS9-P1** at the UMP2/6-311G level. It is worth noting that the comparison of geometries obtained at the UMP2/6-311G level with those at the UMP2/6-311++G(d,p) level shows that the discrepancies are considerably large. For example, both of the forming F···H bond lengths in the two transition structures obtained at the UMP2/6-311G level are about 0.1 Å shorter than that at the UMP2/6-311++G(d,p) level. Likewise, both of the breaking C···H bond lengths in them at a low level are 0.03∼0.04 Å shorter than that at a high level. Fallaciously, the transition state **TS8-P1** is energetically high-lying among the five abstraction hydrogen transition states at the CCSD(T)/cc-pVTZ//UMP2/6-311G level, inconsistent with the results obtained at a higher level of theory (see Table S1, Supporting Information). To rationalize this difference, we turn to the PES features of the hydrogen abstraction processes. The use of the low-level transition state geometry generally gives poor results, and in the five instances, this method actually gives *negative* barriers! "When the low level transition states occurs very late the higher level energy can already have dropped below the energy of the reactants".[37] Furthermore, bearing in mind the limitation (the use of harmonic frequencies for the highly anharmonic intramolecular vibrations) inherent in our calculations and considering Yang and Zhang's suggestion[15] (the 6-311G basis set is insufficient for the title reaction), the CCSD(T)/cc-pVTZ//UMP2/6-311G scheme is unreliable. Expectedly and interestingly, as shown in Figure 1, the distances of H···F are 1.356, 1.373, 1.320, 1.293, and 1.280 Å in **TS8-P1**, **TS9-P1**, **TS10-P2**, **TS11-P3**, and **TS12-P4**, respectively, decreasing gradually, which is in line with the trend of their relative energies except for **TS8-P1**.

Chart 1

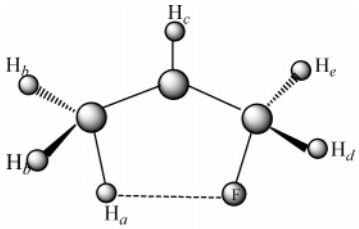

It must be stressed that an exhaustive search on the PES failed to locate a transition structure like that in Chart 1corresponding to a conventional addition−elimination mechanism. Indeed, in previous theoretical studies[21,43] on the reactions of the Cl atom with isoprene and propene, this ringlike transition structure wasn't located on the PESs. Therefore, the addition−elimination mechanism can be safely ruled out from the **F + propene** reaction.

3.2. Experimental Implication. Recently, Ran et al. carried out the kinetic study for the title reaction.[5] In their experiment, three reaction channels were observed: $CH_3 + C_2H_3F$, $H + C_3H_5F$, and $HF + C_3H_5$. They also suggested that the CH_3 formation is the most important channel for this chemical reaction, while both H and HF formation channels are also significant, and a long-lived complex formation is the most important mechanism with some minor contributions from a direct reaction mechanism. However, they did not provide unambiguous information on the site-specific effect in the H-atom elimination channel and the HF formation channel because there are three chemically different hydrogen sites in the propene molecule, although it is important to better understand the roles of different reaction mechanisms in these reaction channels. On the other hand, they did not give any information about the formation of $CH_2F + CH_2{=}CH_2$. In our calculations, it is shown that, among the possible pathways, the most feasible one is that where the atomic radical F and propene approach each other to form the initial weakly bound complex **1** before F addition to the C=C double bond. The elimination of methyl from isomer **3** leads to the main products **P5**, $CH_3 + C_2H_3F$. And, one can find that the atomic radical F directly abstracting the allylic hydrogen of $CH_3CH{=}CH_2$ is the most favorable

pathway, while the abstraction of the vinyl terminal hydrogen should be less competitive in the HF formation channels. Furthermore, the most favorable eliminated H atom is the vinyl inner hydrogen (H_c) after the **F** addition to the vinyl inner carbon in the H formation channels.

Finally, it should be pointed out that, in the title reaction, all of the intermediates and transition states involved in the possible addition−isomerization−elimination channels lie below the reactants. Once the addition reaction proceeds, the reaction system immediately enters a deep potential well. As shown in Figure 2a, the exit barriers are moderately high for all of the addition−isomerization−elimination channels. Undoubtedly, these features will make the formation of long-lived reaction complexes stand a good chance. This is qualitatively consistent with the experimental results.[5]

3.3. Comparison with the Cl + Propene Reaction. To give a deeper understanding of the reaction mechanism of F + propene, it is worthwhile to compare the title reaction with the analogous reaction Cl + propene, which has been extensively studied both experimentally[44−46] and theoretically.[21] One can find that there exists both similarity and discrepancy. In a recent experiment[46] for the **Cl + propene** reaction, Kaiser and Wallington observed experimentally that the addition of a Cl atom to the double bond is the major reaction channel at high pressure (>100 Torr), while at low pressure (<10 Torr), the addition reaction rate slows and the removal of an H atom from the CH_3 group in C_3H_6 is the dominant channel. They suggest that, at lower pressure, the allylic radical may be formed by two processes: (1) a pressure-independent direct abstraction and (2) an addition−elimination process which depends inversely on the total pressure. However, in a recent detailed theoretical investigation, based on the structures on the PESs, Braña and Sordo[21] suggest that the previously established mechanism[44] consisting of direct abstraction and addition−elimination steps is instead made up of addition through an intermediate and two-step abstraction step processes; that is, no direct abstraction mechanism exists on the potential energy surface. They proposed a formally similar general mechanism that can be written as follows:

$$\mathrm{Cl} + \mathrm{C_3H_6} \overset{\mathrm{TS_{abs}}}{\rightleftharpoons} \mathrm{C_3H_5\cdots HCl^*} \rightarrow \mathrm{C_3H_5^\bullet} + \mathrm{HCl} \quad \text{(two-step abstraction)}$$

$$\rightarrow \mathrm{C_3C_5\cdots HCl} \quad \text{(association)}$$

$$\mathrm{Cl} + \mathrm{C_3H_6} \rightleftharpoons \mathrm{C_3H_6\cdots Cl^*} \rightarrow \mathrm{C_3H_5^\bullet\cdots HCl} \xrightarrow{\mathrm{TS_{add}}} \mathrm{C_3H_6Cl^\bullet} \quad \text{(addition)}$$

In general, the potential energy surface features of the two analogous reactions X + propene (X = F and Cl) are very similar. Both reactions involve the same initial association pathway; that is, the halogen atoms and unsaturated hydrocarbons approach each other, forming the initial weakly bound complex before halogen-atom addition to the C=C double bond with no barrier. Furthermore, the types of the five different chemical environments of the H atom picked up by the halogen atoms are identical in the abstraction processes. Theoretically, the allylic hydrogen abstractions by both F and Cl are exergonic processes and involve small barriers. Therefore, both kinetic and thermodynamic considerations support the viabilities of this type of H atom picked up. However, because the F atom with higher electronegativity strongly attracts a lone pair of electrons located at the H atom, the electron density on the H atom is reduced, which leads to an increasing of the reactivity of bond scission between adjacent atoms. Thus, it is obvious that, for the **Cl + propene** reaction, the H-abstraction channel is a two-step abstraction process, while for the **F + propene** reaction, the H-abstraction channel belongs to a direct abstraction mechanism typically. On the other hand, the increasing reactivity of atomic radical F also leads to the mechanism discrepancies as well as the different product distribution between the two reactions. First, for the **Cl + propene** reaction, the product $CH_3 + C_2H_3Cl$ cannot be obtained experimentally. While, for the **F + propene** reaction, the C2−C3 bond cleavage of **I3** to yield the main product $CH_3 + C_2H_3F$ plays an absolute role.[5] Second, for the **Cl + propene** reaction, no literature reported the H-atom formation channel either experimentally or theoretically. However, for the **F + propene** reaction, the H-atom formation channel cannot be neglected because the branching ratio of the $H + C_3H_5$ channel is about 15%. Third, we obtained a new feasible minor product **P6** ($C_2H_4 + CH_2F$), which may play a role in high-temperature ranges for the **F + propene** reaction in this work, while no information about the product ($C_2H_4 + CH_2Cl$) was reported experimentally or theoretically.

Before ending, we would like to make a short comment on the expected behavior of the rate constants at various experimental pressures about the title reaction. As pointed out by Braña and Sordo[21,43] and Kaiser and Wallington[46] on the analogous reactions of **Cl + propene** and **Cl + isoprene**, we conjecture that, for the F + propene reaction, even at high pressure, the activated complexes **I1** and **I*n*** ($n = 8-12$) cannot be stabilized efficiently by third-body collisions as the stabilization energies of these complexes are very small. Taking into account that the **TS1-2**, **TS1-3**, and direct H-abstraction transition states' (**TS8-P1**, **TS9-P1**, **TS10-P2**, **TS11-P3**, and **TS12-P4**) barriers are negligible, there will be no accumulation of **I1** and **I*n*** ($n = 8-12$) ($C_3H_6\cdots F$). As the formation intermediates **I2** and **I3** are exergonic processes and the energy barriers associated with **TS1-2** and **TS1-3** are much lower than that of direct H-abstraction transition states, consequently, the $\mathbf{C_3H_6F^\bullet}$ radical should be the most favored product. Therefore, the major reaction pathways should be the addition−isomerization−elimination reaction channel at the high-pressure limit. At low pressure, the addition−isomerization−elimination reaction rate decreases and the direct hydrogen abstraction reaction becomes the domination channel. Indeed, as a consequence of very small stabilization of **I*n*** (n=8−12) by third-body collisions, $\mathbf{C_3H_5^\bullet}$ production should increase as compared with that obtained under high-pressure conditions. At sufficiently low pressure, the stabilization channel to form the $\mathbf{C_3H_6F^\bullet}$ radical becomes insignificant. In this pressure regime, the rate constant for allyl formation from the direct abstraction channel might be a constant value.

4. Conclusions

A detailed theoretical survey on the complicated doublet PESs of the reaction of atomic radical F with propene, CH_3-$CH{=}CH_2$, has been performed at the UMP2 and CCSD(T) levels of theory. Two different mechanisms and four reaction channels are revealed in the present study. The most competitive reaction channel is the CH_3 radical formation channel. The CH_2F radical formation channel may be more favorable than the H-atom formation channel in high-temperature ranges on the doublet PESs. The pathway Path1 RP5 is the most competitive pathway in the addition−isomerization−elimination reaction mechanism. While in the direct hydrogen abstraction reaction mechanism, the main pathway is Path11 RP1. No addition−elimination mechanism exists on the potential energy surface, which is consistent with previous theoretical studies for the reactions of the Cl atom with propene and isoprene. On the basis of the analysis of the energetics of all channels through which the addition and abstraction reactions proceed, we expect that the actual feasibility of the reaction channels may depend on the reaction conditions in the experiment. Consequently, future experimental studies on the title reaction are highly desirable under various pressures and temperatures. The present work will provide useful information for understanding the processes of atomic radical F reaction with other unsaturated hydrocarbons. Despite the analogous chemical reactivity with the well-known atomic radical Cl, the barrier-free atomic radical F reaction with propene is expected to be of unique importance.

Acknowledgment. This work is supported by the National Natural Science Foundation of China (Nos. 20073014 and 20103003), Excellent Young Teacher Foundation of the Ministry of Education of China, Excellent Young Foundation of Jilin Province, and Technology Development Project of Jilin Province (No. 20050906-6). The authors thank Prof. Jose A. Sordo (Universidad de Oviedo) for helpful discussions. The authors are also thankful for the reviewers' invaluable comments.

Supporting Information Available: Table S1 gives the energies, entropies, enthalpies, and Gibbs free energies. Table S2 shows the vibrational frequencies of the reactant, some important intermediates, transition states, and products. The CCSD(T) single-point energies along the IRC are given in Table S3. This material is available free of charge via the Internet at http://pubs.acs.org.

References

(1) Parson, J. M.; Lee, Y. T. Crossed Molecular Beam Study of $F + C_2H_4$, C_2D_4. *J. Chem. Phys.* **1972**, *56*, 4658−4666.

(2) Parson, J. M.; Shobatake, K.; Lee, Y. T.; Rice, S. A. Unimolecular Decomposition of the Long-Lived Complex Formed in the Reaction $F + C_4H_8$. *J. Chem. Phys.* **1973**, *59*, 1402−1415.

(3) Shobatake, K.; Parson, J. M.; Lee, Y. T.; Rice, S. A. Unimolecular Decomposition of Long-Lived Complexes of Fluorine and Substituted Mono-Olefins, Cyclic Olefins, and Dienes. *J. Chem. Phys.* **1973**, *59*, 1416−1426.

(4) Farrar, J. M.; Lee, Y. T. The Question of Energy Randomization in the Decomposition of Chemically Activated C_2H_4F. *J. Chem. Phys.* **1976**, *65*, 1414−1426.

(5) Ran, Q.; Yang, C.-H.; Lee, Y. T.; Shen, G.; Yang, X. Dynamics of the F Atom Reaction with Propene. *J. Chem. Phys.* **2004**, *121*, 6302−6308.

(6) Ran, Q.; Yang, C. H.; Lee, Y. T.; Shen, G.; Wang, L.; Yang, X. Molecular Beam Studies of the F Atom Reaction with Propyne: Site Specific Reactivity. *J. Chem. Phys.* **2005**, *122*, 044307(1−8).

(7) Manion, J. A.; Tsang, W. Hydrogen Atom Attack on Fluorotoluenes: Rates of Fluorine Displacement. *Isr. J. Chem.* **1996**, *36*, 263−273.

(8) Moehlmann, J. G.; Gleaves, J. T.; Hudgens, J. W.; McDonald, J. D. Infrared Chemiluminescence Studies of the Reaction of Fluorine Atoms with Monosubstituted Ethylene Compounds. *J. Chem. Phys.* **1974**, *60*, 4790−4799.

(9) Zvijac, D. J.; Mukamel, S.; Ross, J. Polarization of the Strongest Rydberg Transitions of 1, 3-Butadiene. *J. Chem. Phys.* **1977**, *67*, 2007−2008.

(10) Hase. W. L.; Bhalla. K. C. A Classical Trajectory Study of the $F + C_2H_4 \rightarrow C_2H_4F \rightarrow H + C_2H_3F$ Reaction Dynamics. *J. Chem. Phys.* **1981**, *75*, 2807−2819.

(11) Clark, D. T.; Scanlan, I. W. A Note on the Transition State of Radical Addition Reactions. *Chem. Phys. Lett.* **1978**, *55*, 102−106.

(12) Kato, S.; Morokuma, K. Potential Energy Characteristics and Energy Partitioning in Chemical Reactions: *Ab Initio* MO Study of $H_2CCH_2F \rightarrow H_2CCHF + H$ Reaction. *J. Chem. Phys.* **1980**, *72*, 206−217.

(13) Schlegel, H. B. Ab Initio Molecular Orbital Studies of Atomic Hydrogen + Ethylene and Atomic Fluorine + Ethylene. 1. Comparison of the Equilibrium Geometries, Transition Structures, and Vibrational Frequencies. *J. Phys. Chem.* **1982**, *86*, 4878−4882.

(14) Schlegel, H. B.; Bhalla, K. C.; Hase W. L. Ab Initio Molecular Orbital Studies of Atomic Hydrogen + Ethylene and Atomic Fluorine + Ethylene. 2. Comparison of the Energetics. *J. Phys. Chem.* **1982**, *86*, 4883−4888.

(15) Zhang, M. B.; Yang, Z. Z. Computational Study on the Reaction $CH_2CH_2 + F \rightarrow CH_2CHF + H$. *J. Phys. Chem. A* **2005**, *109*, 4816−4823.

(16) Robinson, G. N.; Continetti, R. E.; Lee, Y. T. The Translational Energy Dependence of the $F + C_2H_4 \rightarrow H + C_2H_3F$ Reaction Cross Section near Threshold. *J. Chem. Phys.* **1990**, *92*, 275−284.

(17) Harper, W. W.; Nizkorodov, S. A.; Nesbitt, D. J. Quantum State-Resolved Reactive Scattering of $F + CH_4 \rightarrow HF(v,J) + CH_3$: Nascent $HF(v,J)$ Product State Distributions. *J. Chem. Phys.* **2000**, *113*, 3670−3680.

(18) Harper, W. W.; Nizkorodov, S. A.; Nesbitt, D. Differential Scattering Dynamics of $F + CH_4 \rightarrow HF(v,J) + CH_3$ via High-Resolution IR Laser Dopplerimetry. *Chem. Phys. Lett.* **2001**, *335*, 381−387.

(19) Shiu, W.; Lin, J. J.; Liu, K. Reactive Resonance in a Polyatomic Reaction. *Phys. Rev. Lett.* **2004**, *92*, 103201 (1−4).

(20) Lin, J. J.; Zhou, J.; Shiu, W.; Liu, K. State-Specific Correlation of Coincident Product Pairs in the $F + CD_4$ Reaction. *Science* **2003**, *300*, 966−969.

(21) Braña, P.; Sordo, J. A. Theoretical Approach to the Mechanism of Reactions between Halogen Atoms and Unsaturated Hydrocarbons: The Cl + Propene Reaction. *J. Comput. Chem.* **2003**, *24*, 2044−2062.

(22) (a) Frisch, M. J.; Trucks, G. W.; Schlegel, H. B.; Scuseria, G. E.; Robb, M. A.; Cheeseman, J. R.; Zakrzewski, V. G.; Montgomery, J. A., Jr.; Stratmann, R. E.; Burant, J. C.; Dapprich, S.; Millam, J. M.; Daniels, A. D.; Kudin, K. N.; Strain, M. C.; Farkas, O.; Tomasi, J.; Barone, V.; Cossi, M.; Cammi, R.; Mennucci, B.; Pomelli, C.; Adamo, C.; Clifford, S.; Ochterski, J.; Petersson, G. A.; Ayala, P. Y.; Cui, Q.; Morokuma, K.; Malick, D. K.; Rabuck, A. D.; Raghavachari, K.; Foresman, J. B.; Cioslowski, J.; Ortiz, J. V.; Stefanov, B. B.; Liu, G.; Liashenko, A.; Piskorz, P.; Komaromi, I.; Gomperts, R.; Martin, R. L.; Fox, D. J.; Keith, T.; Al-Laham, M. A.; Peng, C. Y.; Nanayakkara, A.; Gonzalez, C.; Challacombe, M.; Gill, P. M. W.; Johnson, B. G.; Chen, W.; Wong, M. W.; Andres, J. L.; Head-Gordon, M.; Replogle, E. S.; Pople, J. A. *Gaussian 98*, revision A.11; Gaussian, Inc.: Pittsburgh, PA, 1998. (b) Frisch, M. J.; Trucks, G. W.; Schlegel, H. B.; Scuseria, G. E.; Robb, M. A.; Cheeseman, J. R.; Montgomery, J. A., Jr.; Vreven, T.; Kudin, K. N.; Burant, J. C.; Millam, J. M.; Iyengar, S. S.; Tomasi, J.; Barone, V.; Mennucci, B.; Cossi, M.; Scalmani, G.; Rega, N.; Petersson, G. A.; Nakatsuji, H.; Hada, M.; Ehara, M.; Toyota, K.; Fukuda, R.; Hasegawa, J.; Ishida, M.; Nakajima, T.; Honda, Y.; Kitao, O.; Nakai, H.; Klene, M.; Li, X.; Knox, J. E.; Hratchian, H. P.; Cross, J. B.; Bakken, V.; Adamo, C.; Jaramillo, J.; Gomperts, R.; Stratmann, R. E.; Yazyev, O.; Austin, A. J.; Cammi, R.; Pomelli, C.; Ochterski, J. W.; Ayala, P. Y.; Morokuma, K.; Voth, G. A.; Salvador, P.; Dannenberg, J. J.; Zakrzewski, V. G.; Dapprich, S.; Daniels, A. D.; Strain, M. C.; Farkas, O.; Malick, D. K.; Rabuck, A. D.; Raghavachari, K.; Foresman, J. B.; Ortiz, J. V.; Cui, Q.; Baboul, A. G.; Clifford, S.; Cioslowski, J.; Stefanov, B. B.; Liu, G.; Liashenko, A.; Piskorz, P.; Komaromi, I.; Martin, R. L.; Fox, D. J.; Keith, T.; Al-Laham, M. A.; Peng, C. Y.; Nanayakkara, A.; Challacombe, M.; Gill, P. M. W.; Johnson, B.; Chen, W.; Wong, M. W.; Gonzalez, C.; Pople, J. A. *Gaussian 03*, revision C02; Gaussian, Inc.: Wallingford, CT, 2004.

(23) Schlegel, H. B. Potential Energy Curves Using Unrestricted Møller−Plesset Perturbation Theory with Spin Annihilation. *J. Chem. Phys.* **1986**, *84*, 4530−4534.

(24) Sponer, J.; Hobza, P. J. Interaction Energies of Hydrogen-Bonded Formamide Dimer, Formamidine Dimer, and Selected DNA Base Pairs Obtained with Large Basis Sets of Atomic Orbitals. *J. Phys. Chem. A* **2000**, *104*, 4592−4597.

(25) Nguyen, M. T.; Creve, S.; Vanquickenborne, L. G. Difficulties of Density Functional Theory in Investigating Addition Reactions of the Hydrogen Atom. *J. Phys. Chem.* **1996**, *100*, 18422−18425.

(26) Gonzalez, C.; Schlegel, H. B. Reaction Path following in Mass-Weighted Internal Coordinates. *J. Phys. Chem.* **1990**, *94*, 5523−5527.

(27) Purvis, G. D.; Bartlett, R. J. A Full Coupled-Cluster Singles and Doubles Model: The Inclusion of Disconnected Triples. *J. Chem. Phys.* **1982**, *76*, 1910−1918.

(28) Dunning, T. H., Jr. Gaussian Basis Sets for Use in Correlated Molecular Calculations. I. The Atoms Boron through Neon and Hydrogen. *J. Chem. Phys.* **1989**, *90*, 1007−1023.

(29) Ignatyev, I. S.; Xie, Y.; Allen, W. D.; Schaefer, H. F. Mechanism of the $C_2H_5 + O_2$ Reaction. *J. Chem. Phys.* **1997**, *107*, 141−155.

(30) Schlegel, H. B.; Sosa, C. Ab Initio Molecular Orbital Calculations on $F + H_2 \rightarrow HF + H$ and $OH + H_2 \rightarrow H_2O + H$ Using Unrestricted Møller−Plesset Perturbation Theory with Spin Projection. *Chem. Phys. Lett.* **1988**, *145*, 329−333.

(31) McDouall, J. J. W.; Schlegel, H. B. Analytical Gradients for Unrestricted Hartree−Fock and Second-Order Møller−Plesset Perturbation Theory with Single Spin Annihilation. *J. Chem. Phys.* **1989**, *90*, 2363−2369.

(32) Farnell, L.; Pople, J. A. Radom, L. Structural Predictions for Open-Shell Systems: A Comparative Assessment of ab Initio Procedures. *J. Phys. Chem.* **1983**, *87*, 79−82.

(33) Sekusak, S.; Liedl, K. R.; Sabljic, A. Reactivity and Regioselectivity of Hydroxyl Radical Addition to Halogenated Ethenes. *J. Phys. Chem. A* **1998**, *102*, 1583−1594.

(34) Schlegel, H. B. Potential Energy Curves Using Unrestricted Møller−Plesset Perturbation Theory with Spin Annihilation. *J. Chem. Phys.* **1986**, *84*, 4530−4534.

(35) Stanton, J. F. On the Extent of Spin Contamination in Open-Shell Coupled-Cluster Wave Functions. *J. Chem. Phys.* **1994**, *101*, 371−374.

(36) Sosa, C.; Schlegel, H. B. Calculated Barrier Heights for OH + C_2H_2 and OH + C_2H_4 Using Unrestricted Moeller−Plesset Perturbation Theory with Spin Annihilation. *J. Am. Chem. Soc.* **1987**, *109*, 4193−4198.

(37) Malick, D. K.; Petersson, G. A.; Montgomery, J. A., Jr. Transition States for Chemical Reactions I. Geometry and Classical Barrier Height. *J. Chem. Phys.* **1998**, *108*, 5704−5713.

(38) Huber, K. P.; Herzberg, G. Constants of Diatomic Molecules. In *NIST Chemistry WebBook, NIST Standard Reference Database Number 69*; Linstrom, P. J., Mallard, W. G., Eds.; National Institute of Standards and Technology: Gaithersburg, MD, 2005; p 20899. http://webbook.nist.gov (accessed Jun 2006). Data prepared by J. W. Gallagher and R. D. Johnson, III.

(39) Lide, D. R.; Christensen, D. An Improved Structure Determination for Vinyl Fluoride. *Spectrochim. Acta* **1961**, *17*, 665−668.

(40) Ochsenfeld, C.; Kaiser, R. I.; Lee, Y. T. A Coupled-Cluster *ab Initio* Study of Triplet C_3H_2 and the Neutral−Neutral Reaction to Interstellar C_3H. *J. Chem. Phys.* **1997**, *106*, 4141−4151 and references therein.

(41) Geng, C. Y.; Li, J. L.; Huang, X. R.; Sun, C. C. A Barrier-Free Atom−Molecule Reaction: F + HONO *Chem. Phys.* **2006**, *324*, 474−482. (b) Li, J. L.; Geng, C. Y.; Huang, X. R.; Sun, C. C. Atomic Radical-Molecule Reactions F + $CH_3C{\equiv}CH$: Mechanistic Study. *Theor. Chem. Acc.* (accepted).

(42) Coxon, J. A.; Hajigeorgiou, P. G. Isotopic Dependence of Born−Oppenheimer Breakdown Effects in Diatomic Hydrides: The $B^1\Sigma^+$ and $X^1\Sigma^+$ States of HF and DF. *J. Mol. Spectrosc.* **1990**, *142*, 254−278.

(43) Braña, P.; Sordo, J. A. Mechanistic Aspects of the Abstraction of an Allylic Hydrogen in the Chlorine Atom Reaction with 2-Methyl-1,3-Butadiene (Isoprene). *J. Am. Chem. Soc.* **2001**, *123*, 10348−10353.

(44) Stutz, J.; Ezell, M. J.; Ezell, A. A.; Finlayson-Pitts, B. J. Rate Constants and Kinetic Isotope Effects in the Reactions of Atomic Chlorine with *n*-Butane and Simple Alkenes at Room Temperature. *J. Phys. Chem. A* **1998**, *102*, 8510−8519.

(45) Pilgrim, J. S.; Taatjes, C. A. Infrared Absorption Probing of the Cl + C_3H_6 Reaction: Rate Coefficients for HCl Production between 290 and 800 K. *J. Phys. Chem. A* **1997**, *101*, 5776−5782.

(46) Kaiser, E. W.; Wallington, T. J. Pressure Dependence of the Reaction Cl + C_3H_6. *J. Phys. Chem.* **1996**, *100*, 9788−9793.

CT050233M